FOR REFERENCE

NOT TO BE TAKEN FROM THIS ROOM

NACA

RESEARCH MEMORANDUM

VIBRATION SURVEY OF BLADES IN 10-STAGE

AXIAL-FLOW COMPRESSOR

I - STATIC INVESTIGATION

By André J. Meyer, Jr. and Howard F. Calvert

Lewis Flight Propulsion Laboratory
Cleveland, Ohio

CLASSIFICATION CANCELLED

Authority J. W. Crowley Date 4/14/53

2010501

By H-I-19-54 See naca

RF 2014

NATIONAL ADVISORY COMMITTEE
FOR AERONAUTICS

WASHINGTON
January 31, 1949

NACA RM No. E8J22   ~~RESTRICTED~~

NATIONAL ADVISORY COMMITTEE FOR AERONAUTICS

RESEARCH MEMORANDUM

VIBRATION SURVEY OF BLADES IN 10-STAGE

AXIAL-FLOW COMPRESSOR

I - STATIC INVESTIGATION

By André J. Meyer, Jr. and Howard F. Calvert

SUMMARY

An investigation was conducted to determine the cause of failures in the seventh- and tenth-stage blades of an axial-flow compressor. The natural frequencies of all rotor blades were measured and critical-speed diagrams were plotted. These data show that the failures were possibly caused by resonance of a first bending-mode vibration excited by a fourth order of the rotor speed in the seventh stage and a sixth order in the tenth stage.

INTRODUCTION

Several experimental jet-propulsion engines were constructed in which the six-stage axial-flow compressor of the engine was replaced with a ten-stage axial-flow compressor to increase thrust output. The other components of the engine were relatively unchanged. During thrust-stand tests conducted by the manufacturer, several blade failures occurred in early experimental 10-stage compressors.

The NACA Lewis laboratory conducted an investigation to determine the cause and to find, if possible, a means of preventing the blade failures in this engine. The first part of the investigation consisted in statically measuring the natural frequencies of each blade in the compressor and comparing these frequencies with possible exciting forces. First bending-, second bending-, and first torsional-mode frequencies were measured in all stages; second torsional- and third and fourth bending-mode frequencies were determined only in the first stage. The node shapes of higher modes of vibration were determined in an attempt to correlate the position of high-stress points for the various modes with the location of actual failures.

APPARATUS AND PROCEDURE

The apparatus used to obtain the natural frequencies of the compressor blades is shown in figure 1. The blades, made from a magnetic material, are susceptible to excitation by an electromagnetic coil. Power for the coil used for this purpose was supplied by amplifying an oscillator signal.

The coil was held near the end of the blade, perpendicular to the blade surface, and at a distance sufficient to prevent the blade from striking the core during resonance. The frequency of excitation was varied until high amplitudes were observed. The appearance of a high amplitude indicated that resonance had been obtained, and the natural frequency of the blade was then read directly from the oscillator dial. First bending-, second bending-, and first torsional-mode frequencies were measured in all stages; second torsional- and third and fourth bending-mode frequencies were determined only in the first stage. The total error involved in making the frequency measurements was less than 2 percent.

Small granules of ordinary table salt were sprinkled on a blade vibrating at one of its natural frequencies to outline the sand pattern of the nodes (fig. 2). A violin bow and the magnetic coil were used to excite the blades in obtaining the node patterns.

DISCUSSION AND RESULTS

According to the engine manufacturer, blade failures had occurred in six different engines operating within the speed range of 16,000 to 17,000 rpm at high pressure ratios. The exact speeds of the various engines at the time of failure are unknown except in one case in which the engine was running at 16,600 rpm. In each case only one blade broke and the fracture always occurred in either the seventh or tenth stage of the compressor. The fractures occurred 3/16 to 1/4 inch from the periphery of the rotor disk; fatigue had started at the point of maximum thickness on the convex side of the blade.

Blade failure in only the seventh and tenth stages of the compressors definitely indicates that the failures are caused by vibratory stresses inasmuch as all the blades of the sixth, seventh, and eighth stages are the same in shape and size except for the amount trimmed from the end of the blade. The ninth- and tenth-stage blades are also similar to each other except in length. The engines were operated at the rated speed of 17,000 rpm, approximately 400 rpm above

651

the speed at which the blades failed; hence, the failures cannot be attributed to stress rupture caused by centrifugal force.

Natural-Frequency Measurements

Because all the failures occurred within the narrow speed range of 16,000 to 17,000 rpm, the blades were possibly excited at their resonant point. The fundamental natural frequency was therefore measured for each blade; these data as well as the highest, lowest, and average frequencies observed in each stage are listed in table I. A 20-percent variation in blade frequencies existed in any single stage; if the rotor spins at rated speed, the frequencies of all blades might approach the highest frequency in the stage because the centrifugal force and the thermal expansion raise the frequency by tightening the bulbous blade root. The centrifugal force also has a stiffening effect on the blades, which increases the frequency from 72 percent in the first stage to 16 percent in the tenth stage above the static measurements. Several blades in the ninth and tenth stages were loose but would act like firmly clamped blades when the compressor was in operation.

Second bending- and first torsional-mode vibrations were easily excited in all stages; their frequencies were measured and are recorded in table II. Only in the eighth stage was the frequency of the second bending mode higher than the frequency of the first torsional mode. No reason for this exception was determined.

Node Locations

The location of failure and the starting point of fatigue made it necessary to know the stress patterns for all modes of vibration in order to determine the modes that could cause the failure. High-stress points are located at positions of greatest change in slope of the deflection curve for the vibrating blade; the greatest slope changes generally occur at the antinode points. In addition to the antinode at the tip of the blades, the other antinodes are located approximately midway between nodes. The high-stress points were estimated from sand patterns shown in figures 2 to 8. All of the nodes, except the one at the root and the one closest to the tip of the blade, are points of zero stress. Application of this analysis to the sand pattern shown in figure 4, for example, indicates that a high-stress point would be located (1) at the root, (2) about two-thirds the distance from the root to the nearest node because the root is fixed, not hinged, and (3) at some point between the node nearest the root and the tip of the blade. Low stresses occur at a

position about one-third the distance from the root to the nearest
node for the third bending-mode vibration photographed. This
position is approximately the location of failure in the seventh
and tenth stages when distances are proportioned according to total
blade length. Consequently, in bending vibration only the first or
second modes could cause the failures. In the torsional modes of
vibration (figs. 3 and 5), the maximum-stress areas indicated by the
node position are located at the leading and trailing edges near the
blade root. Theoretically, the maximum stress for an airfoil-shaped
bar is along the maximum blade thickness provided that the ends are
permitted to warp at will. When the blade is rigidly restrained,
however, the maximum-stress regions originate at the leading and trail-
ing edges near the root and shift toward the center of the chord farther
along the length of the blade. This conclusion was verified by data
obtained from numerous resistance-wire strain gages cemented near a
blade root in three directions of orientation, and by fatigue failing
several blade specimens in torsion with a pneumatic vibrator. Torsional
modes can therefore be disregarded because torsion would result in
fatigue starting at the leading and trailing edges rather than at the
maximum blade thickness. The node shapes on the blades of the seventh
and ninth stages are distorted and the torsional modes therefore must
be considered (fig. 8). The significance of the torsional modes might
be more accurately evaluated from strain-gage data taken during engine
operation.

Critical-Speed Diagrams

The natural frequencies existing in each of the 10 stages of
the compressor rotor, plotted on semilogarithmic grid to emphasize
the more easily excited modes of vibration, are shown in the critical-
speed diagrams of figure 9. The highest first bending-mode frequency
corrected for the effect of centrifugal force is used for all diagrams.
The exciting forces caused by wakes from the front-bearing-support
arms and the stator blades and the effect of the split compressor case
are shown plotted against rotor speed. The intersections of the curves
of the natural frequencies and of those of the exciting-force frequen-
cies indicate the critical speeds at which blade vibration resonance
can be expected. Intersections below 14,000 rpm are ignored because
extended operation of the engine is accomplished only at high speeds
and the low speeds are quickly passed when starting the engine.

A critical speed of 14,400 rpm is indicated on figure 9(a) at a
third bending-mode vibration excited in the first-stage rotor blades
by the 22 stator blades immediately following. High modes of vibration
such as the third bending mode are difficult to excite and are there-
fore probably not serious. This critical speed is the only one readily
apparent in the compressor.

Within the operating range of the engine, the exciting force required to cause a resonant vibration in the seventh-stage blades in the first bending mode is approximately the fourth order of the rotor speed (fig. 9(g)). The only fourth-order exciting force obviously present in the compressor is caused by the four arms supporting the front main bearing but it is doubtful that the effect of the arms would carry through as far as the seventh stage. In the tenth stage, the resonant point of first bending-mode vibrations at 16,600 rpm coincides exactly with a sixth-order excitation (fig. 9(j)). The blades are possibly being mechanically or aero-dynamically excited but no exciting force of these orders could be determined. All the failures reported occurred in complete engines and, although a compressor has been operated at various speeds up to 17,000 rpm in an NACA test cell for more than 450 hours, no failures have occurred. Some coupling effect might possibly take place between the turbine or the accessories and the compressor during complete engine operation. Operation at high pressure ratios may also produce the air-flow velocities and pressure conditions necessary to excite blade flutter.

SUMMARY OF RESULTS

Results of an investigation to determine the reason for failure of blades of the seventh and tenth compressor stages in the 10-stage axial-flow compressor at a speed of 16,600 rpm indicated a possibility of exciting first bending-mode vibrations in the seventh-stage blades by a fourth-order excitation of the rotative speed. The tenth-stage blades were possibly excited in the first bending mode by a sixth-order excitation.

Another possible source of excitation was the existence of an aerodynamic condition causing a flutter form of blade vibration.

Lewis Flight Propulsion Laboratory,
    National Advisory Committee for Aeronautics,
        Cleveland, Ohio.

TABLE I

FUNDAMENTAL NATURAL FREQUENCIES OF BLADES ON COMPRESSOR ROTOR

Blade	Natural frequencies (cps) Stages									
	1	2	3	4	5	6	7	8	9	10
1	386	492	556	560	726	758	920	1076	1158	1400
2	378	484	526	620	712	774	884	1128	1376	1390
3	416	478	570	616	702	802	936	964	1030	1540
4	382	474	544	588	690	802	936	1000	1276	1470
5	400	490	476	604	734	804	910	1056	1204	1480
6	386	488	494	586	742	796	899	1084	984	1430
7	394	486	548	566	724	808	974	1120	1270	1470
8	374	502	514	626	780	754	990	1040	1280	1470
9	394	498	480	622	732	814	882	980	1116	1220
10	394	498	506	574	654	778	900	1120	1136	1390
11	400	486	512	588	696	814	930	1116	1150	1370
12	398	498	522	598	716	796	922	1100	1116	1470
13	386	494	484	574	700	808	880	1016	1240	1330
14	380	474	522	594	694	792	888	1090	976	1320
15	372	514	512	578	686	784	890	1052	1150	1420
16	412	476	468	576	690	826	908	974	1060	1450
17	362	466	526	556	680	774	944	1070	1120	1440
18	376	472	494	594	764	808	928	1060	1154	1220
19	396	480	512	572	742	810	940	1026	1300	Loose
20	392	422	506	564	750	806	918	1080	1230	1200
21	380	486	524	568	714	780	856	1020	1240	Loose
22	390	468	466	582	724	794	882	1050	1100	Loose
23	392	454	500	630	718	800	880	1020	1200	Loose
24			502	568	714	716	902	1100	1160	1560
25			522	574	736	824	918	1080	1030	Loose
26			524	588	764	786	886	1106	1132	Loose
27			484	610	650	804	922	1062	1242	1210
28			498	610	688	774	930	1088	1110	1380
29			516	566	712	796	900	1090	1180	1350
30			536	584	682	788	944	1082	1100	1440
31			504	596	696	764	880	1090	1220	1410
32			514	568	686	778	892	1146	1000	1360
33					738	814	968	1080	1040	1320
34					696	816	920	1100	1244	1430
35						806	906	1040	1160	1480
36						822	900	1070	1204	1390
37						810	914	1052	1300	1360
38						794	900	1052	1080	1380
39						762	956	1039	1280	1530
40						770	918	1096	1070	1330
41						804	922	1118	1380	1370
42						820	910	968	1090	1480
43						790	898	1060	1220	1530
44							920	1114	1090	1450
45							916	1012	1030	1430
46								1028	1190	1420
47								1134	1070	1380
48									1120	1440
49									1080	1440
50									1090	1410
51									1230	1430
52									1140	1430
53									1070	1470
54									1120	1450
55									1020	1450
56									1170	1250
57									1140	1400
58									1240	1270
59									1050	1400
60									1210	1320
61									1100	1260
62									1090	1280
63									1140	1250
64									1180	1400
65									1250	1380
66									1120	1510
67									1150	1280
68									1180	1450
69									1140	1380
70									1040	1360
71									1150	1450
72									Loose	1350
73									Loose	1510
74									Loose	1420
75									1060	1410
76									1130	1450
77									1080	1390
78									1120	1340
Highest	416	514	570	630	764	826	980	1146	1380	1510
Lowest	352	422	466	556	650	718	856	964	976	1200
Average	388	481	511	586	712	793	913	1065	1146	1384

TABLE II - NATURAL FREQUENCIES OF VARIOUS

MODES OF BLADE VIBRATION

Stage	Blade	Natural frequencies (cps)		
		Vibration mode		
		First bending	Second bending	First torsional
1	7	394	1940	2820
2	7	486	2520	3000
3	8	514	2640	3240
4	8	626	3380	3660
5	8	750	3780	3900
6	10	778	3920	4340
7	10	900	4440	4780
8	10	1120	5660	5180
9	18	1154	5420	6160
10	18	1220	5000	6920

NACA
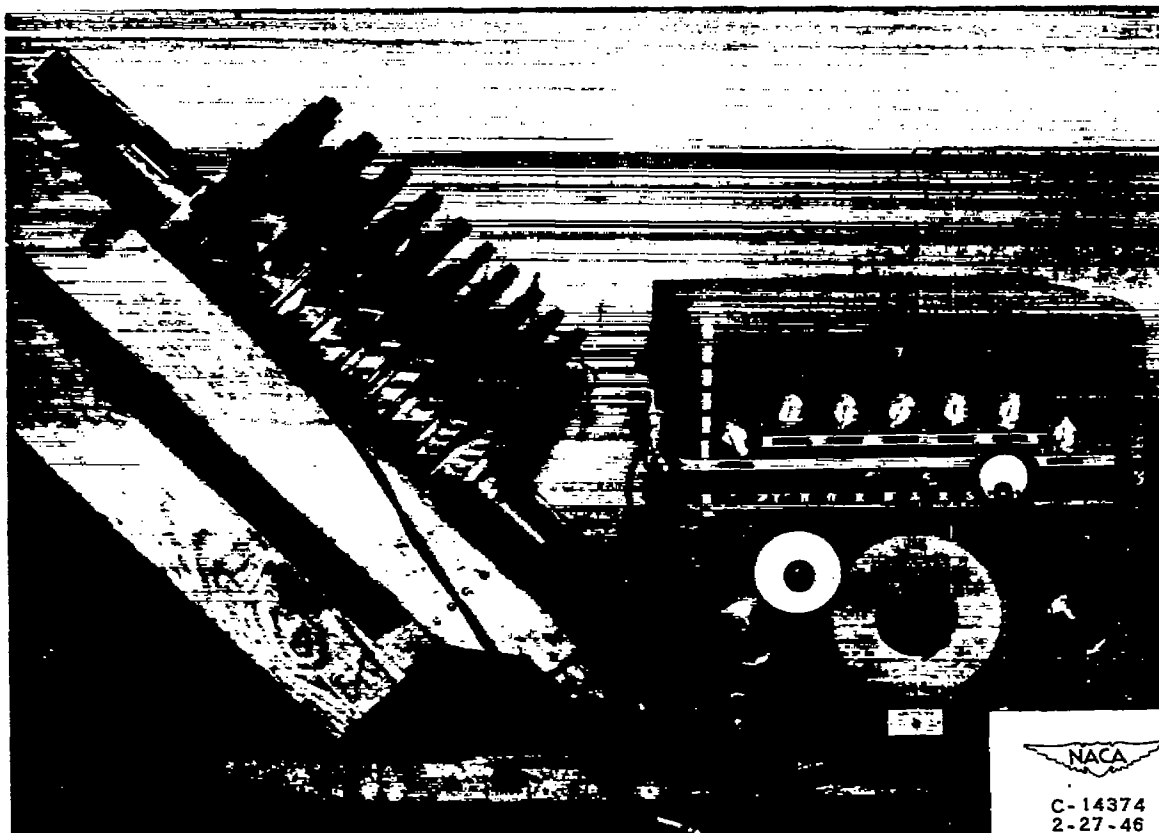
Figure 1. - Electromagnetic coil, amplifier, and oscillator used to determine natural
frequencies of compressor blades.

Figure 2. - Sand pattern for second bending-mode vibration on first-stage blade. Frequency of vibration, 1940 cycles per second.

C-14377
2-27-46
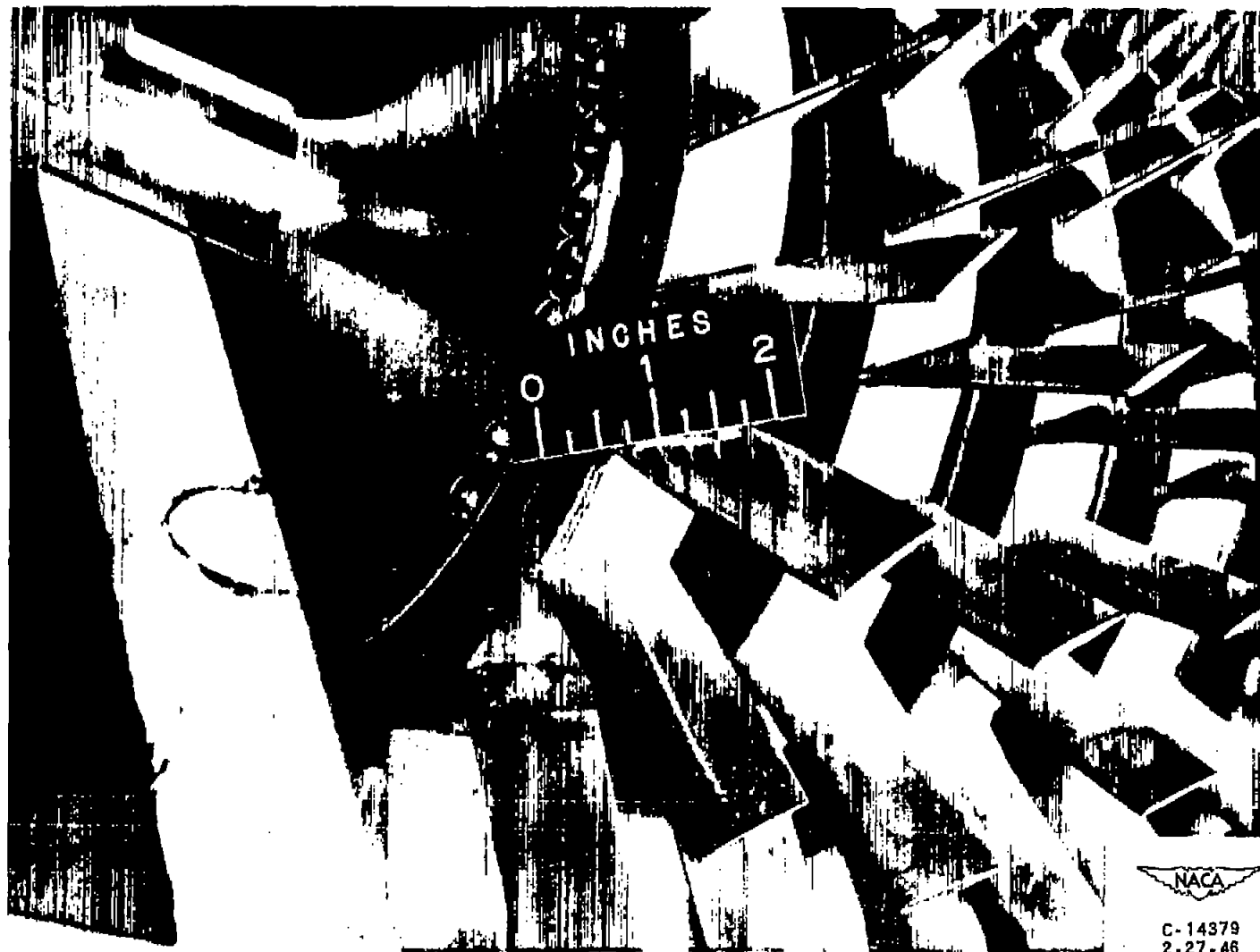
Figure 3. - Sand pattern for first torsional-mode vibration on first-stage blade. Frequency of vibration, 2820 cycles per second.
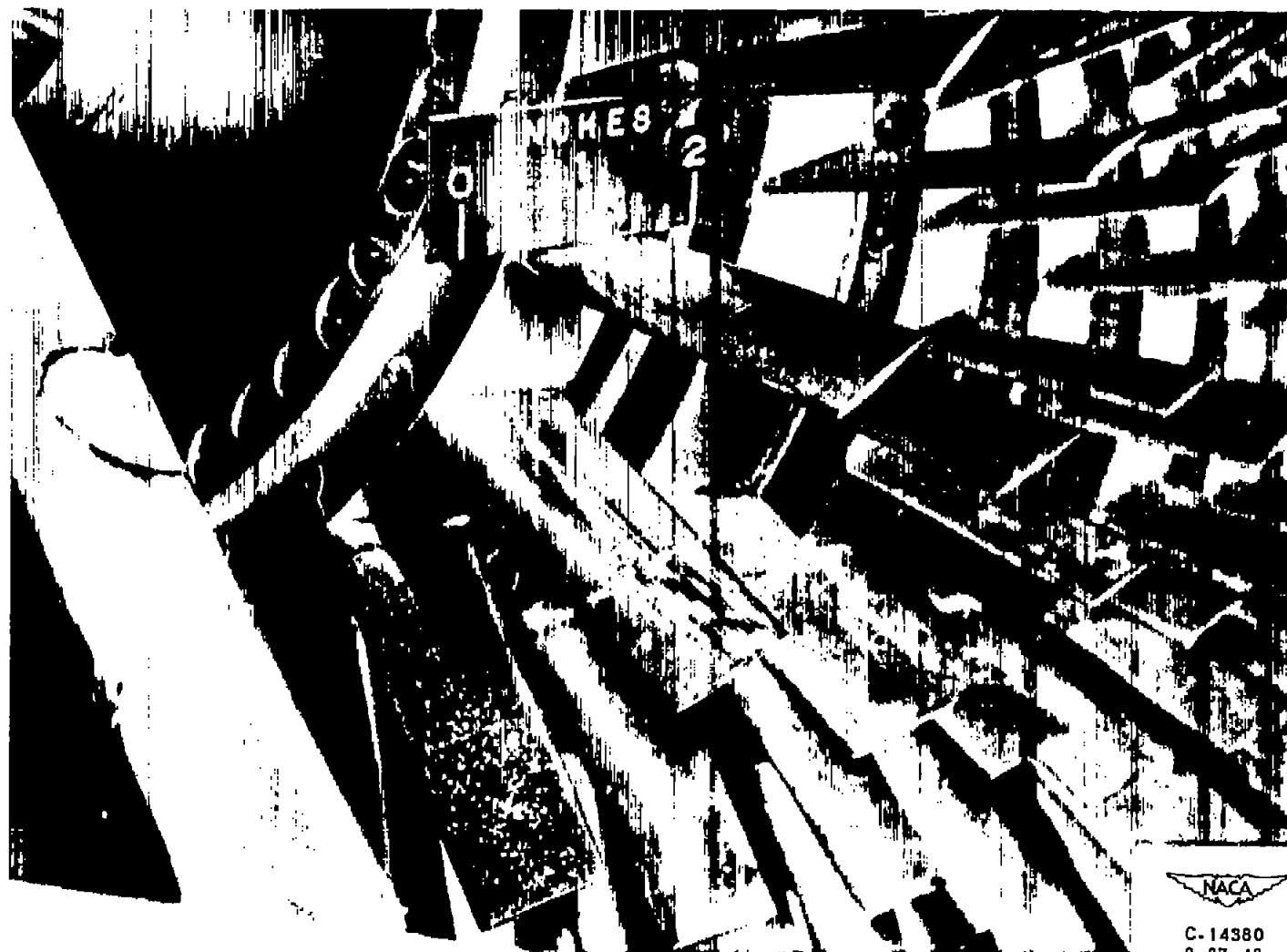
Figure 5. - Sand pattern for second torsional-mode vibration on first-stage blade. Frequency of vibration, 6840 cycles per second.
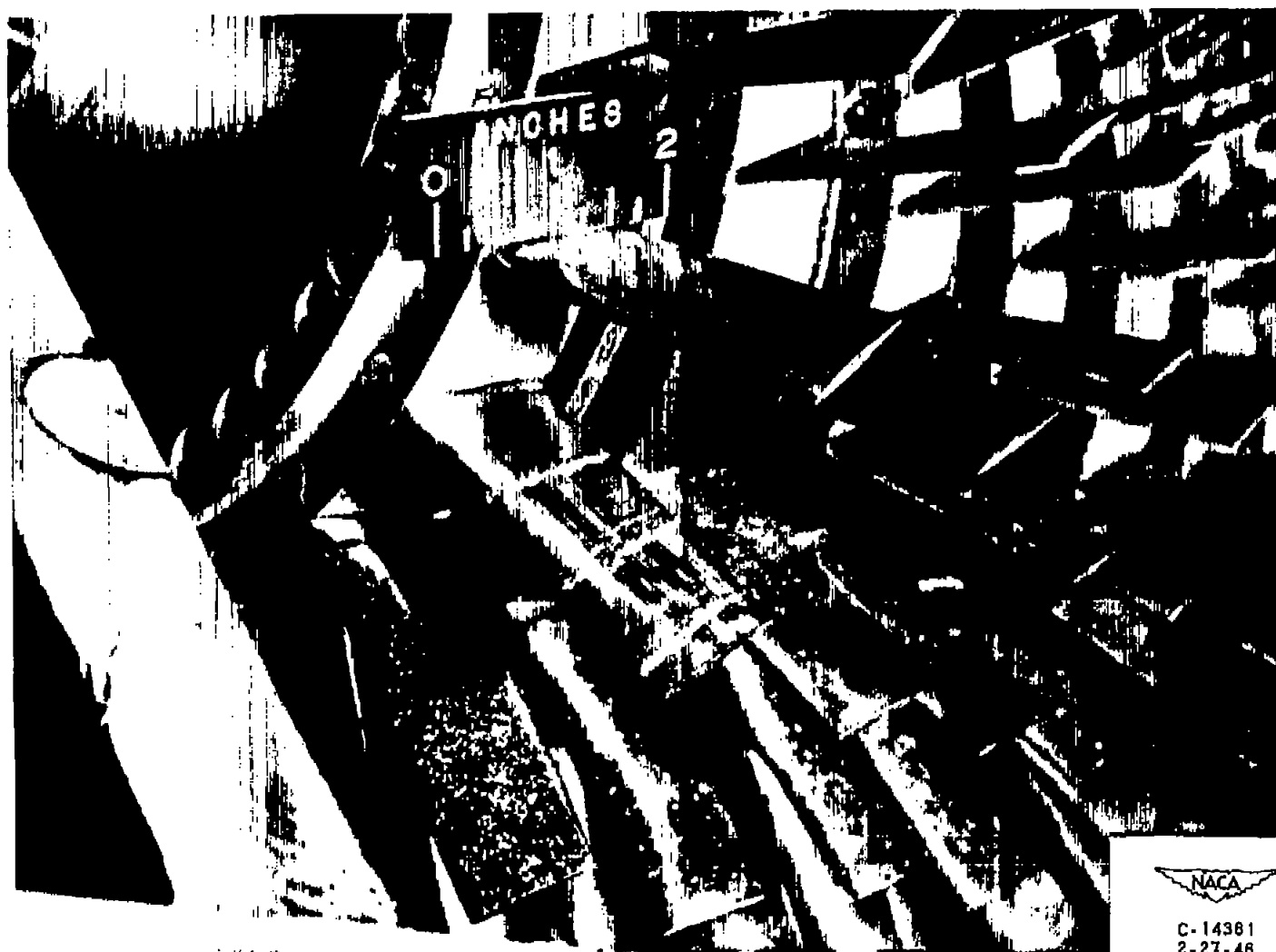
Figure 6. - Sand pattern for fourth bending-mode vibration on first-stage blade. Frequency of vibration, 9600 cycles per second.

Figure 7. - Sand pattern for second bending-mode vibration on seventh-stage blade showing distorted node shape. Frequency of vibration, 4440 cycles per second.

Figure 8. - Sand pattern for first torsional-mode vibration on ninth-stage blade showing distorted node shape. Frequency of vibration, 6160 cycles per second.
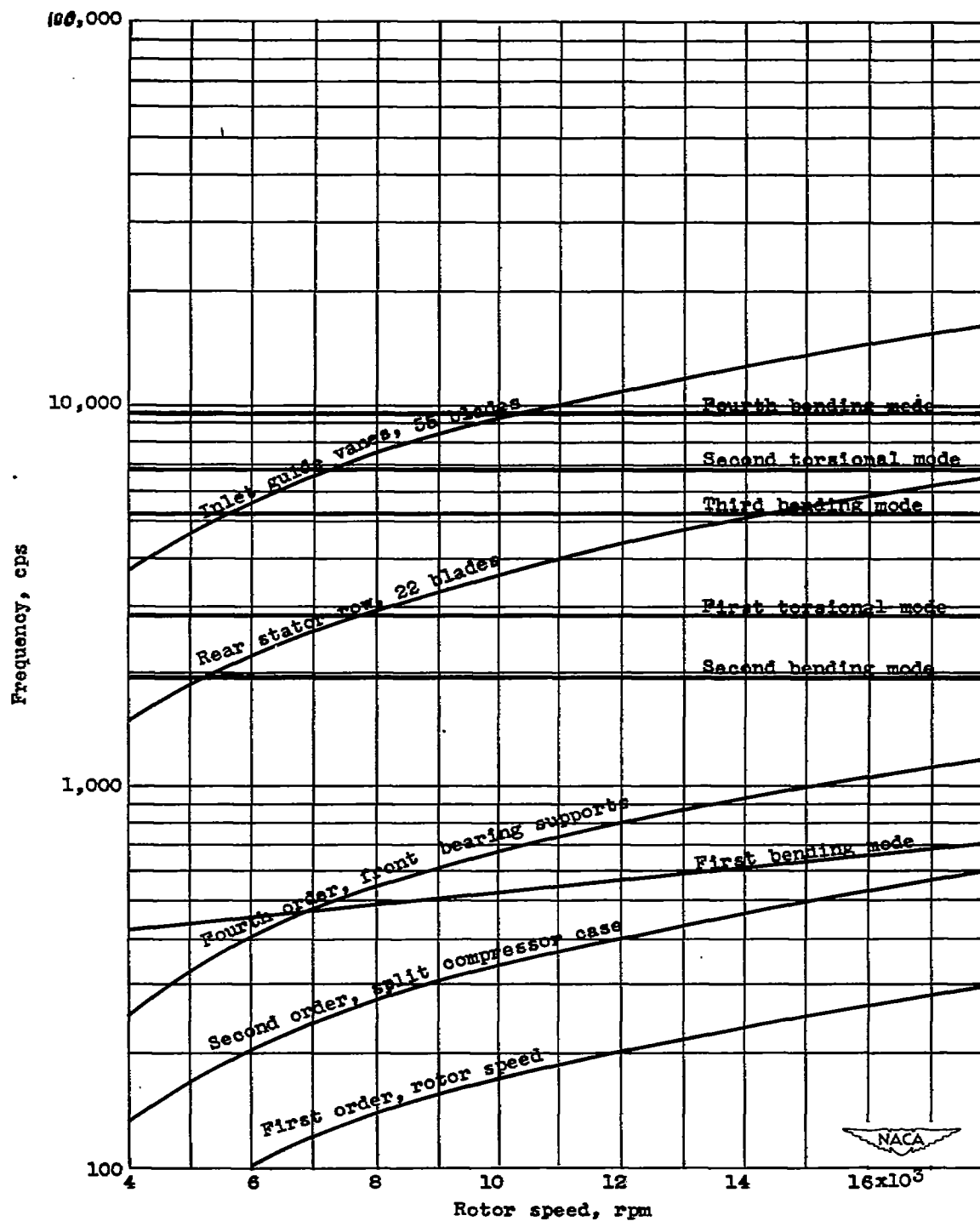
(a) First stage.

Figure 9. – Critical-speed diagrams for 10 stages of compressor rotor.
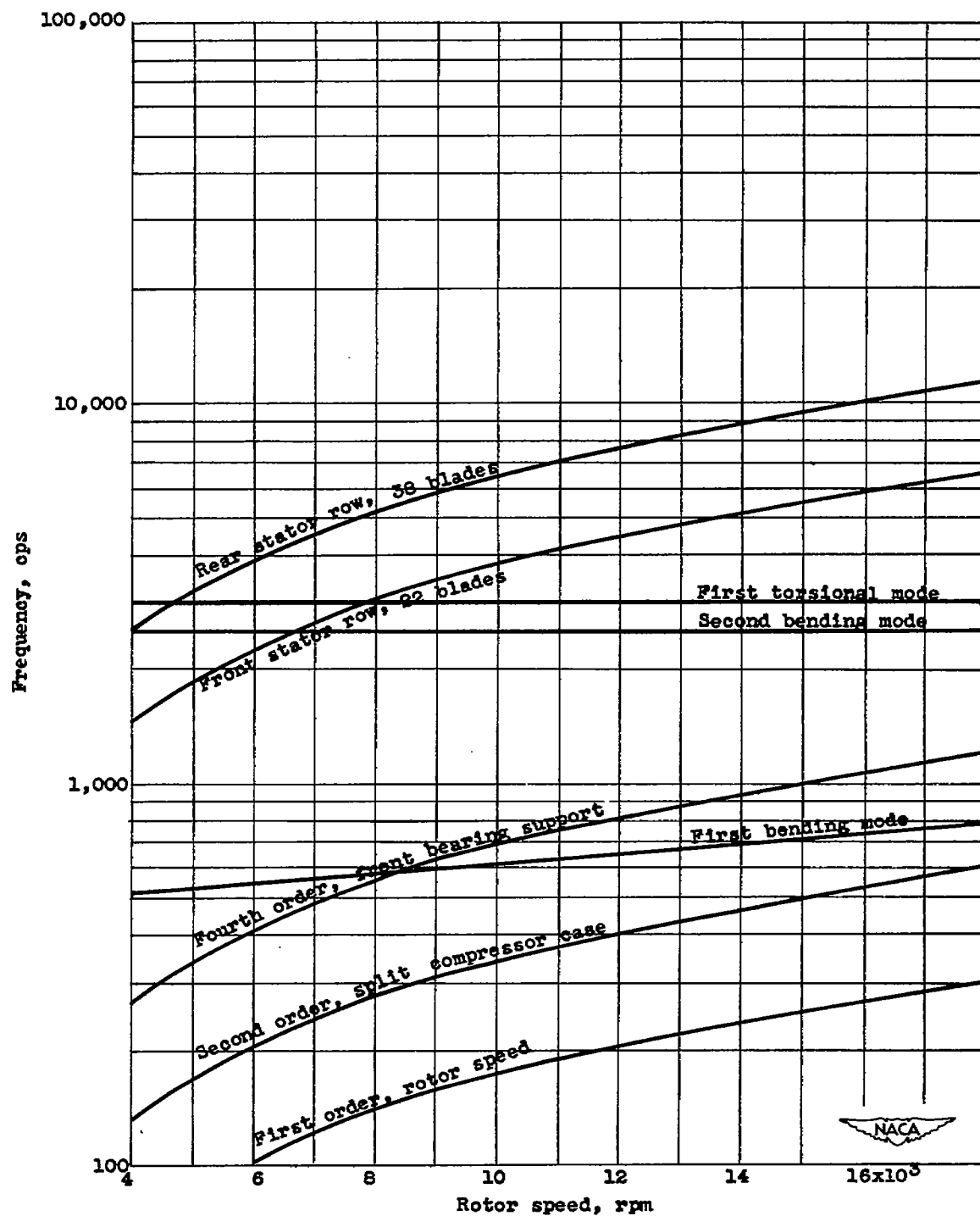
(b) Second stage.

Figure 9. - Continued.   Critical-speed diagrams for 10 stages of
                          compressor rotor.
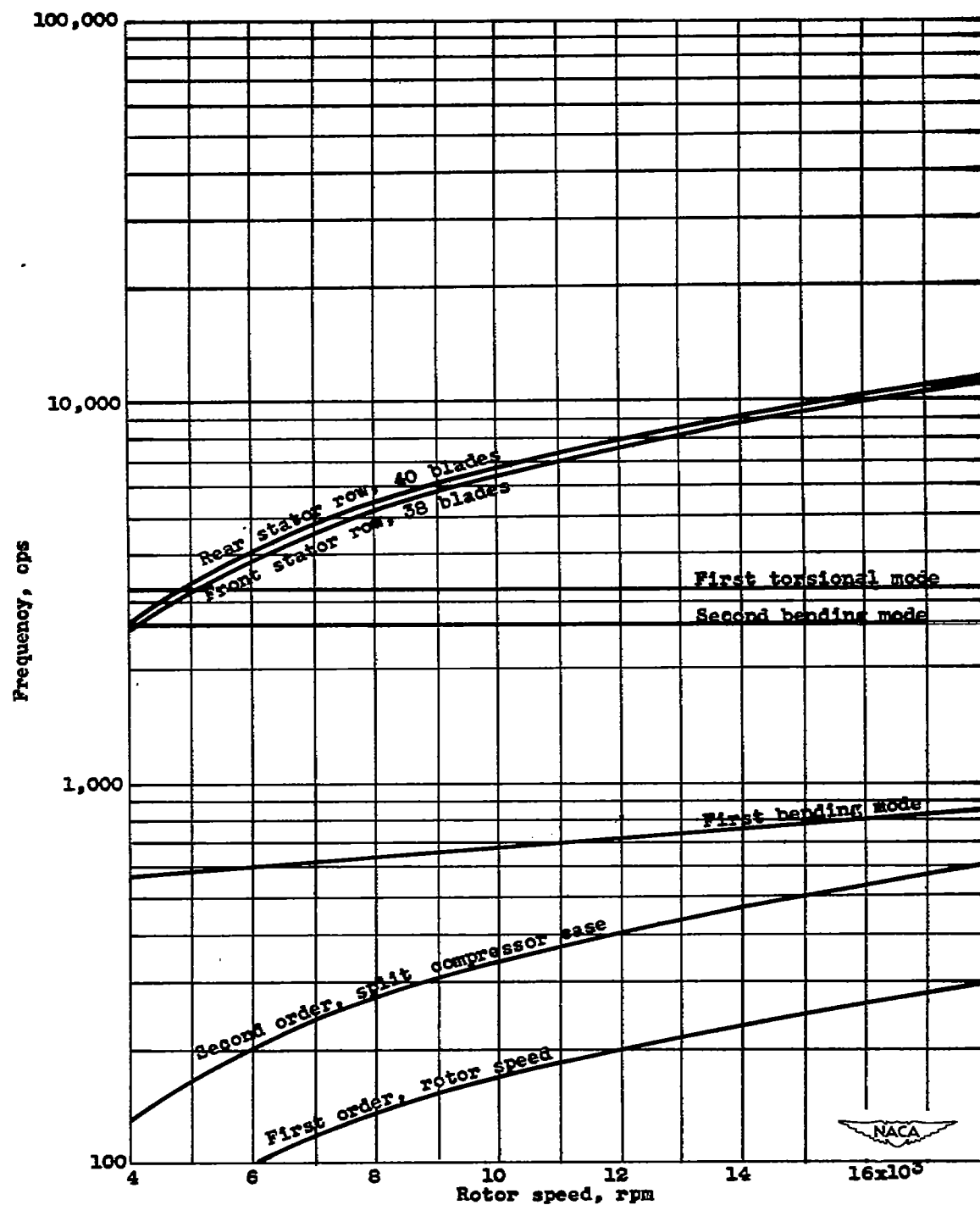
(c) Third stage.
Figure 9. - Continued.   Critical-speed diagrams for 10 stages of
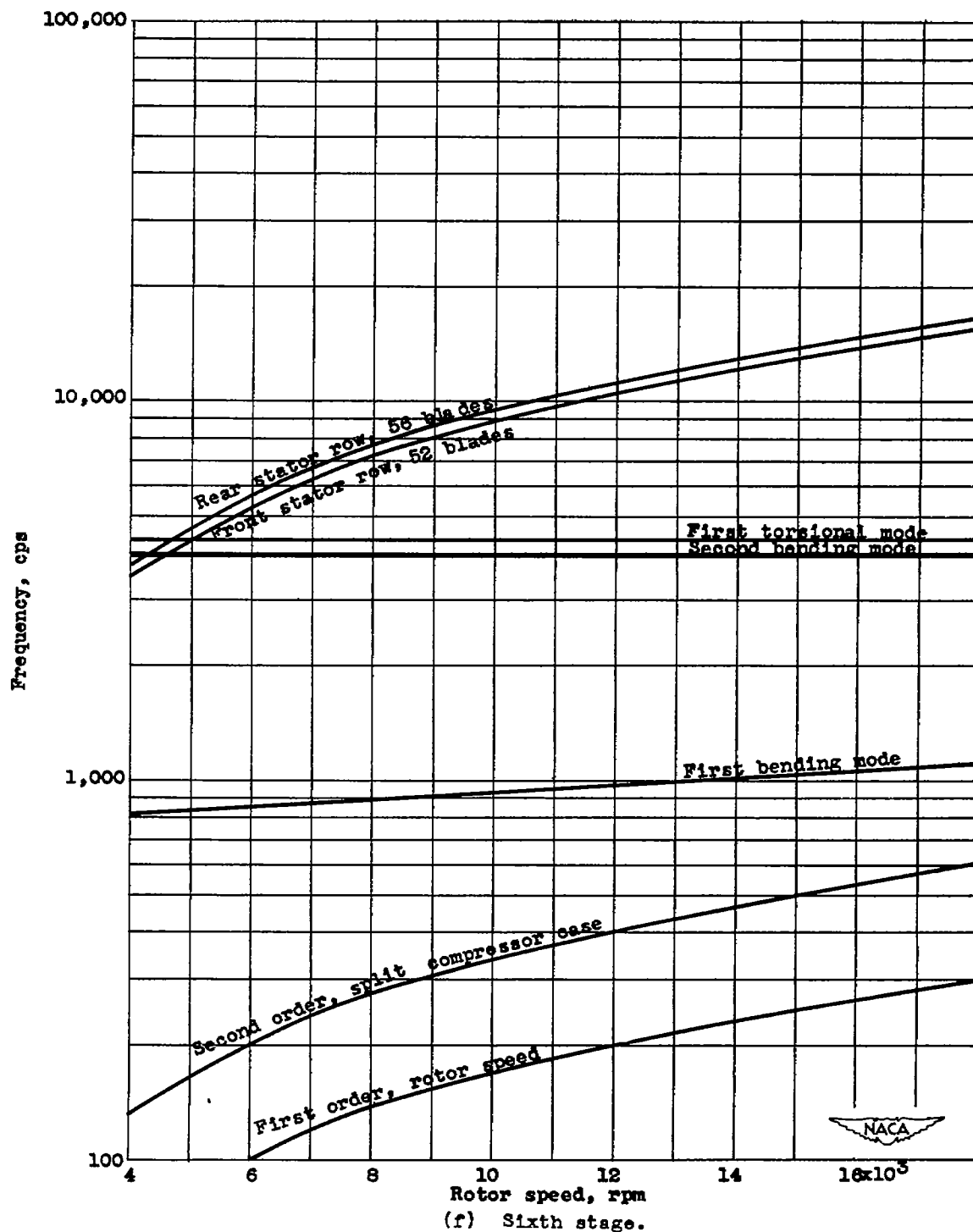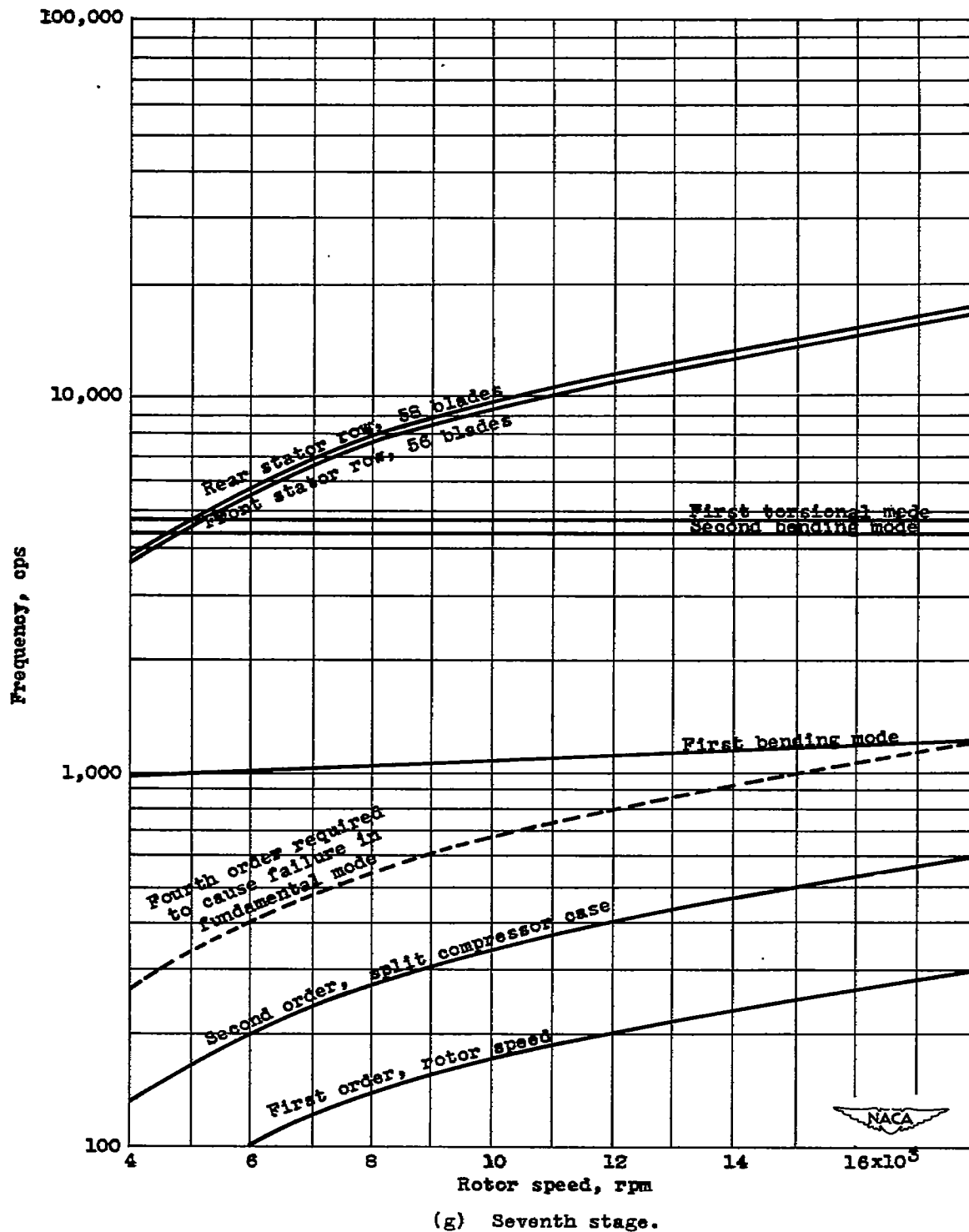compressor rotor.
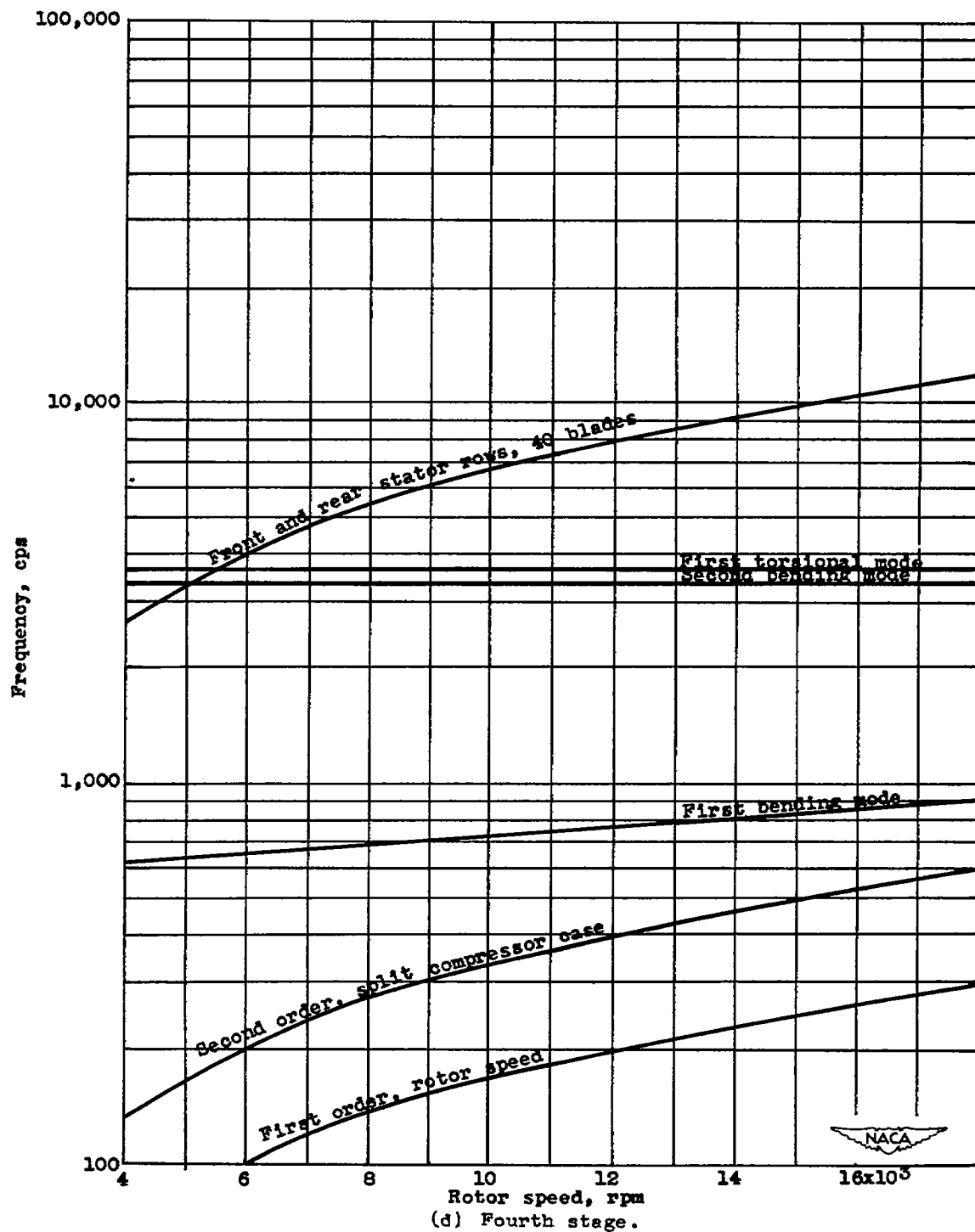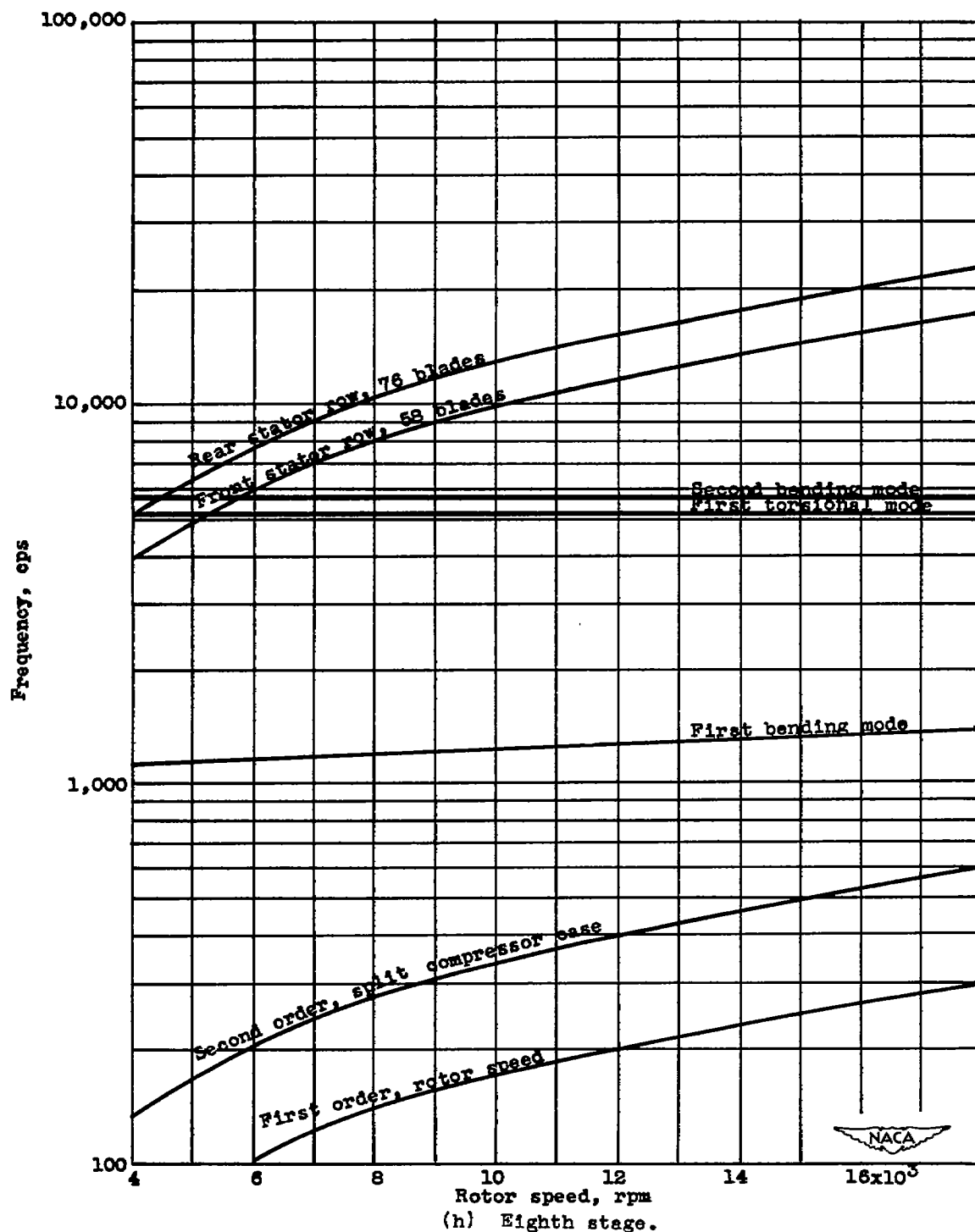
(d) Fourth stage.

Figure 9. - Continued. Critical-speed diagrams for 10 stages of
compressor rotor.

651

(e) Fifth stage.

Figure 9. – Continued. Critical-speed diagrams for 10 stages of
compressor rotor.

651

(f) Sixth stage.

Figure 9. - Continued. Critical-speed diagrams for 10 stages of compressor rotor.

(g)   Seventh stage.

Figure 9. - Continued.   Critical-speed diagrams for 10 stages of
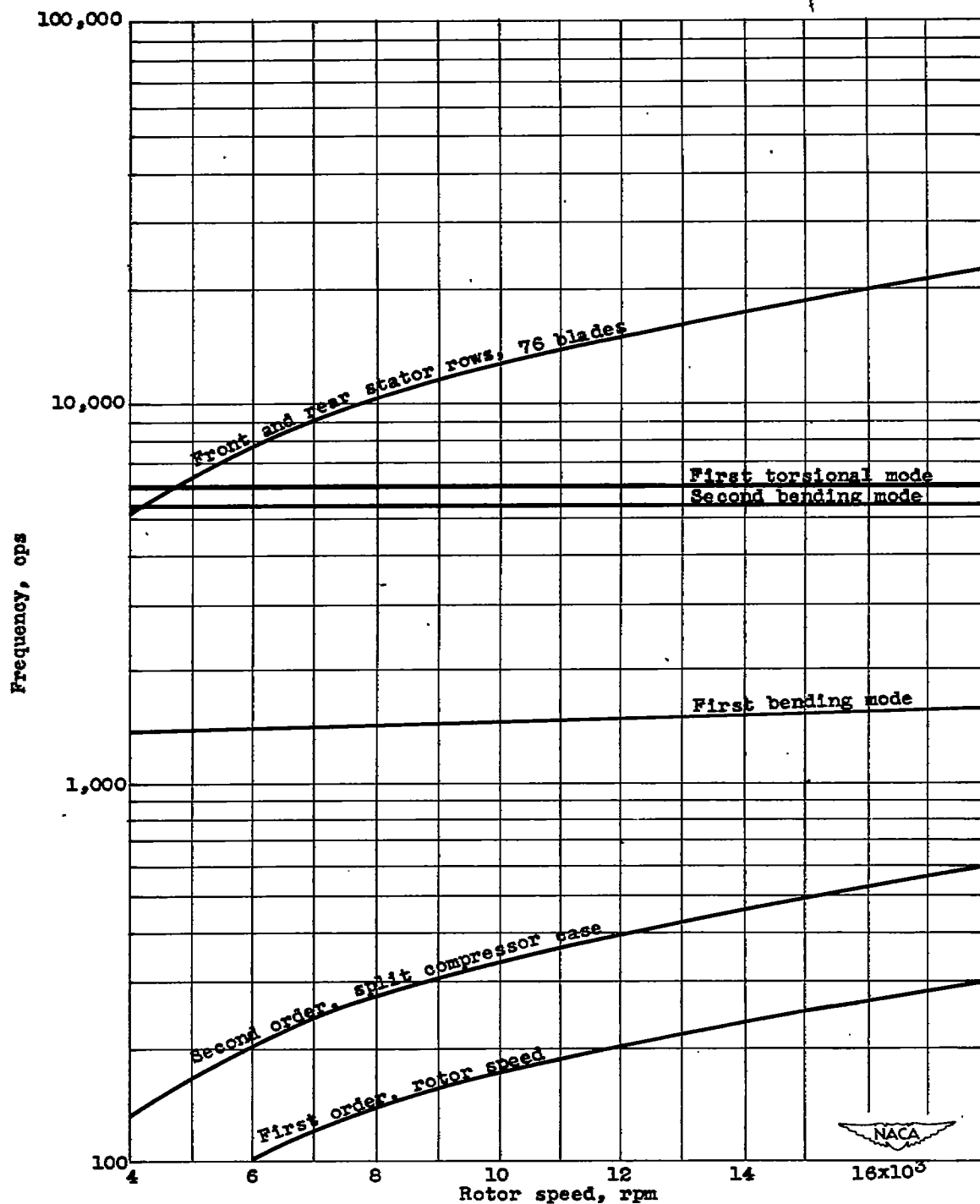compressor rotor.

(h) Eighth stage.

Figure 9. - Continued.   Critical-speed diagrams for 10 stages of
compressor rotor.

(1) Ninth stage.

Figure 9. - Continued.   Critical-speed diagrams for 10 stages of
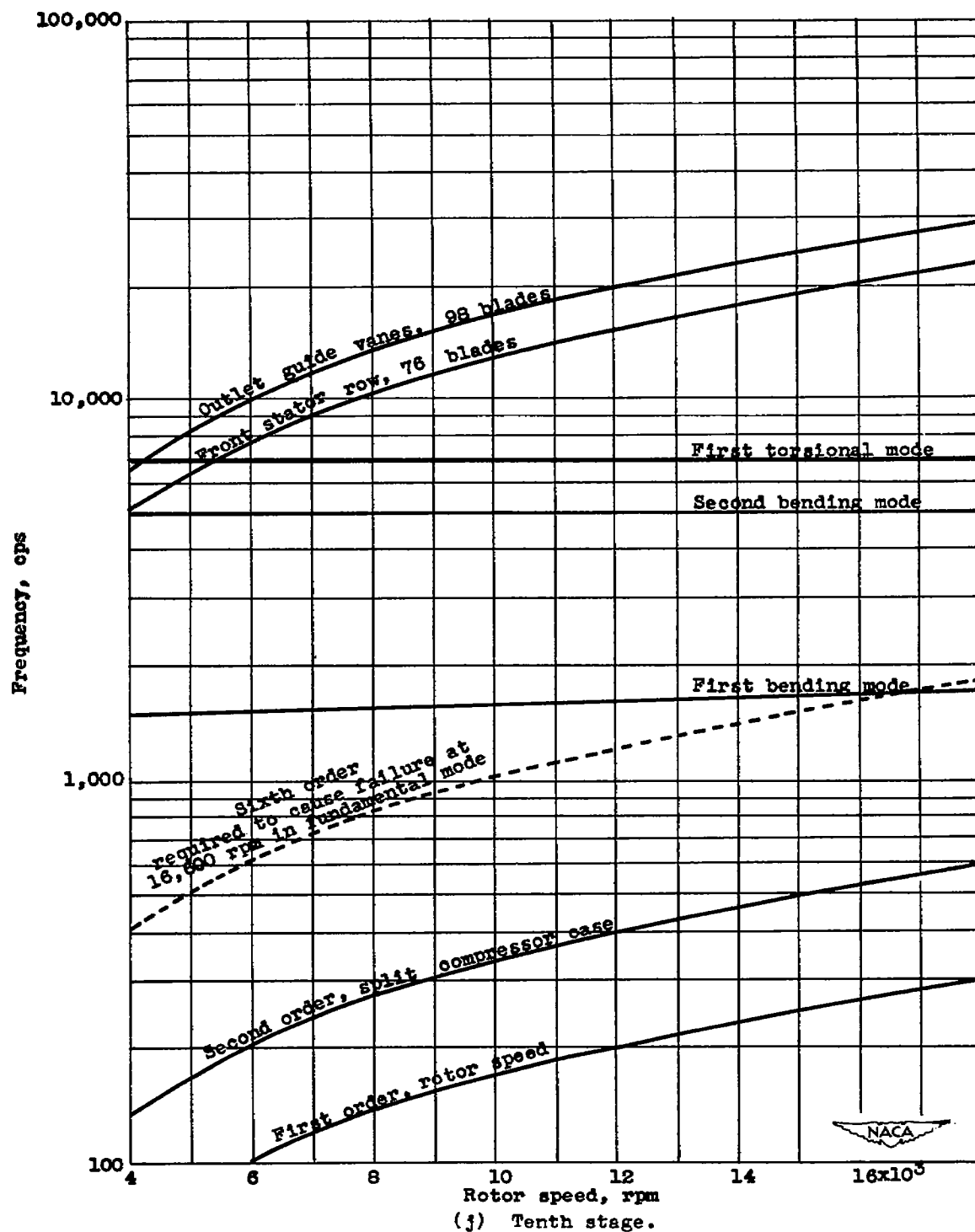compressor rotor.

(j) Tenth stage.

Figure 9. - Concluded.   Critical-speed diagrams for 10 stages of
compressor rotor.